Generation of tunable FSK millimeter-wave using photonic mixer for 5G wireless applications in NR FR2 band

ANU SHEETAL[1], HARJIT SINGH[1], HARMINDER SINGH[2], AMIT GROVER[3], MEET KUMARI[4,*], REECHA SHARMA[5]

[1]*Department of Engineering and Technology, Guru Nanak Dev University Regional Campus, Gurdaspur, Punjab, India*
[2]*Department of Mechanical Engineering, Guru Nanak Dev University, Amritsar, Punjab, India*
[3]*Department of Electronics and Communication Engineering, Shaheed Bhagat Singh State University, Ferozepur, Punjab, India*
[4]*Department of ECE, UIE and UCRD, Chandigarh University, Mohali-140413, Punjab, India*
[5]*Department of Electronics and Communication Engineering, Punjabi University Patiala, Punjab, India*

In this paper, a novel approach for the generation of tunable 5 Gb/s frequency shift keying (FSK) millimeter-wave (mm-wave) upto 60 GHz using photonic mixers is proposed. Here, the FSK mm-wave is tuned at 2.5 and 5 Gb/s with 10, 20 and 30 GHz radio frequency (RF) clock using a single drive Mach-Zehender modulator (MZM) biased at null and quadrature points of the transmission curve. The results show that a high power narrowband 40 and 60 GHz electrical signals have also beneficently generated from 20 and 30 GHz RF clock respectively to accomplish 5G applications in FR2 mm-wave band (24.25- 52.6 GHz).

(Received September 16, 2024; accepted April 3, 2025)

Keywords: 5G, FSK, MM-WAVE, MZM, NRFR2 BAND, Photonic mixer

1. Introduction

The up gradation of the mobile and wireless networks from fourth generation (4 G) to fifth generation (5G) is progressing at a rapid pace to deal with the enormous advanced applications in today's scenario. The 5G wireless systems use existing 4 G or new radio (NR) frequency bands: frequency ranges 1 and 2 (FR1 and FR2) for advanced wireless and mobile applications. FR1 consists of sub-6 GHz frequency bands (typically 600, 700, 800, 900, 1500, 2100, 2300 and 2600 MHz) conventional applications and new definite usages like internet of things (IoT), industrial automation as well as business. FR2 commonly known as millimeter-wave (mm-wave) range that consists of frequency bands in range of 24.25-52.6 GHz offering the widest harmonization with ultra-high-speed communication, the lowest latencies in the spectrum and minimized user equipment complexity. Also, wireless access network (WAN) at mm-wave band (30 to 300 GHz) has huge bandwidth which offers a substitute for fast indoor or hotspot links to be used for 5 G applications developing new opportunities for backhaul/ fronthaul network in licensed and unlicensed spectrum. Currently researchers are working on 5 G wireless communication by introducing technologies offering small cell opinions with enhanced network speed and capacity [1,2].

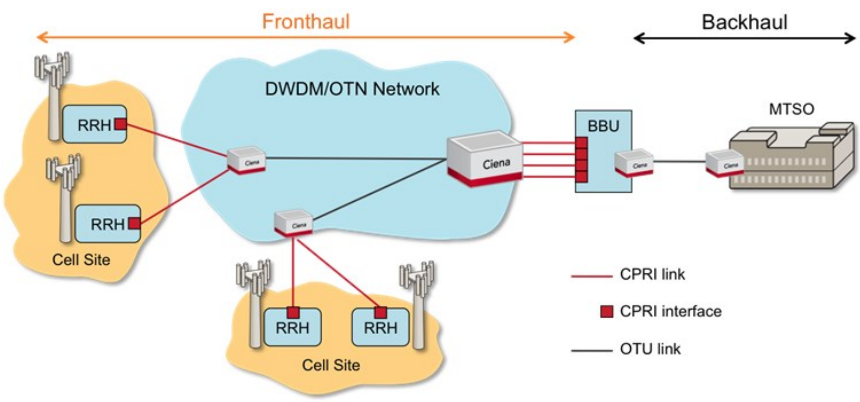

Fig. 1. Setup of 5 G fronthaul and backhaul mm-wave network (colour online)

Fig. 1 shows the basic architecture of fronthaul and backhaul 5G network in its easiest form. Here, backhaul model joins the portable devices to the wired network through backhauling the traffic over physically separated cell spots via baseband unit (BBU) to mobile switching telephone offices (MTSOs). In fronthaul, radio unit (RU) equipment is considered as a remote radio head (RRH) and is positioned at cell spot. The BBU is located at the center in the cell site to serve multiple RRHs. The optical transmission unit (OTU) provides optical connections that connect the centralized BBU along with the multiple RRHs. The BBU processes end user as well as control data, however the RRH offers radio signal transmission over the free space via antennas. Common Public Radio Interface (CPRI) is a standardized protocol which handles these fronthaul channels and is compatible with various optical transceivers from other common substantial layer standards, like 1000Base-SX/LX Ethernet (IEEE 802.3-2002), Fiber Channel (INCITS revision 8, FC-PI-4), 10GBase-LX4 Ethernet (IEEE 802.3-2005), 10GBase-S/L/E 10G Ethernet (IEEE 802.3-2008) etc. CPRI also helps in keeping the network cost effective while facilitating optical link engineering. To assist the small cells as well as and mm-wave for upcoming 5G networks, optical communication plays a significant part in fronthaul and backhaul networks. Thus, optical access network (OAN) is essential for scalability and assisting the projected 5 G implementation goals by 2023: 1-10 Gb/s at the user end; 100 Gb/s for backhaul network; 1 Tb/s and 1Pb/s for metro and core networks respectively. For realization of optical transport link in the 5 G backhaul and fronthaul networks, microwave photonics uses optical devices to produce and process mm-waves in light domain. MW photonics helps to minimize the bandwidth bottleneck of electrical devices in the network [1]. In recent years, the photonic mixers are utilized in a various application such as military radar, base station, radio-over fiber (RoF) systems, satellite communication phased, array beam forming and wireless communications etc. [2–4].

Compared with the conventional electric mixer, mm-wave photonic mixer has the benefits of huge bandwidth, low loss, less weight, and resistance to electromagnetic interference (EMI). RF photonic mixer is a three-port active or passive equipment that changes the frequency (up-conversion or down-conversion) of the electromagnetic signal though preserving phase and amplitude features of initial signal to allow amplification of received signal at an intermediate frequency (IF) [5,6].

In the previous work, a photonic generation of phase-code microwave signal in optical domain to minimize the system complexity, improve the RF signal and reduce the bandwidth congestion of electrical devices is proposed in the network [7]. The generation of microwave band using suppressed carrier amplitude shift keying (ASK) signal with dual-drive Mach-Zehnder modulators (MZMs) having unbalanced amplitudes is demonstrated [8]. The concept of wavelength switched optical RF frequency comb generation with 100 ps transitions to obtain distinct frequency shift keying (FSK) signals by applying line spectral shaping technique is presented [9]. A model for photonic generation of mm-wave FSK signal utilizing distinct delay interference in the two polarization areas of optical polarization modulated short pulses is presented [10].

Recently, photonic-assisted mm-wave signals with distinct modulation formats, consisting of ASK, phase shift keying (PSK), amplitude differential PSK (ADPSK), quadrature amplitude modulation (QAM) and quaternary PSK (QPSK) signals became most admired schemes specifically by utilizing single or dual-drive MZMs [11]. Furthermore, from the comprehensive literature review it is noted that although much work has been reported for optical microwave FSK generation, but the generation of millimeter-wave still needs to be explored and realized for NR FR2 mm-wave frequency band for 5 G applications [12]. In [11], a wavelength selective switches based on silicon microring resonators is designed at 10 Gbps throughput at maximum 25 GHz frequency for wavelength division multiplexing (WDM) based application but at high cost. In [13] and [14], a Fourier domain mode-locked opto-electronic oscillator and joint radar and communication complex and costly designs are realized for ASK/FSK and binary PSK (BPSK) modulation respectively, for 5 G based radar applications. In [15], a 20Gbps signals with 60 GHz frequency is designed for complementary metal oxide semiconductor (CMOS) technology. In [4], a ASK mm-wave based 100 GHz frequency based system at 10 Gbps presented for gas sensing applications.

The fifth generation communications demand a multi Gbps traffic rate in its small cells. In this respect, mm-wave RF signals are the optimal decisions to be used for high-speed throughput. Generation of mm-wave frequency RF signals is critical in electrical domain thus; photonic generation of these signals is more efficient. Again, wireless access networks operating at mm-wave bands (30-300 GHz) incorporates large bandwidth and offers a substitute for high-speed indoor communication for 5G services [16]. Therefore, in this paper, a novel scheme to obtain tunable FSK millimeter-wave using a single drive MZM biased at null as well as quadrature points of transmission curve for ‘0’ and ‘1’ bits respectively, has been proposed. Using this scheme, FSK signals from 20 to 60 GHz have been efficiently generated to accomplish 5 G applications in FR2 millimeter-wave band (24.25- 52.6 GHz).

In Section 2, the basic principle and mathematical modeling for photonic FSK mm-wave generation using microwave photonic mixer (MPM) is given. Section 3 explains the system description of tunable FSK millimeter-wave generation using MPM by varying bit rate (2.5-10 Gb/s) and RF frequency (10-30GHz). In Section 4, results have been analyzed as well as discussed with the help of optical and electrical spectra. Finally, the conclusions have been drawn in Section 5.

2. Principle and mathematical modeling of MPM based millimeter-wave FSK generation

The FSK is one of the fundamental modulation schemes used in communication systems like telemetry, caller ID, radio-sounds and many more. In this scheme, binary information is sent through distinct frequency variations of the carrier signal as shown in Fig. 2. The binary FSK (BFSK) uses two different frequencies to transmit logic 0 and 1 bits where space frequency corresponds to bit '0' and mark frequency denotes bit'1'. Mm-wave FSK signal is obtained by using a single drive MZM which acts as a MPM. Here, an electrical unipolar ASK baseband signal is mixed with RF clock having angular frequency $\omega_f = (2\pi f)_{RF}$. The output of the mixer is added with an on-off keying (OOK) signal to generate the final millimeter-wave FSK signal using electrical-to-optical modulation (EOM) with single drive MZM.

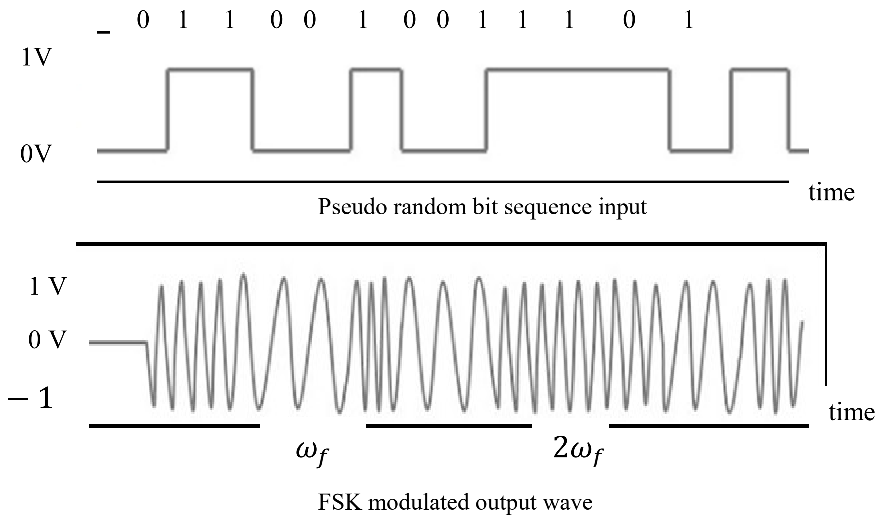

Fig. 2. Wave shapes of the generated M FSK signal

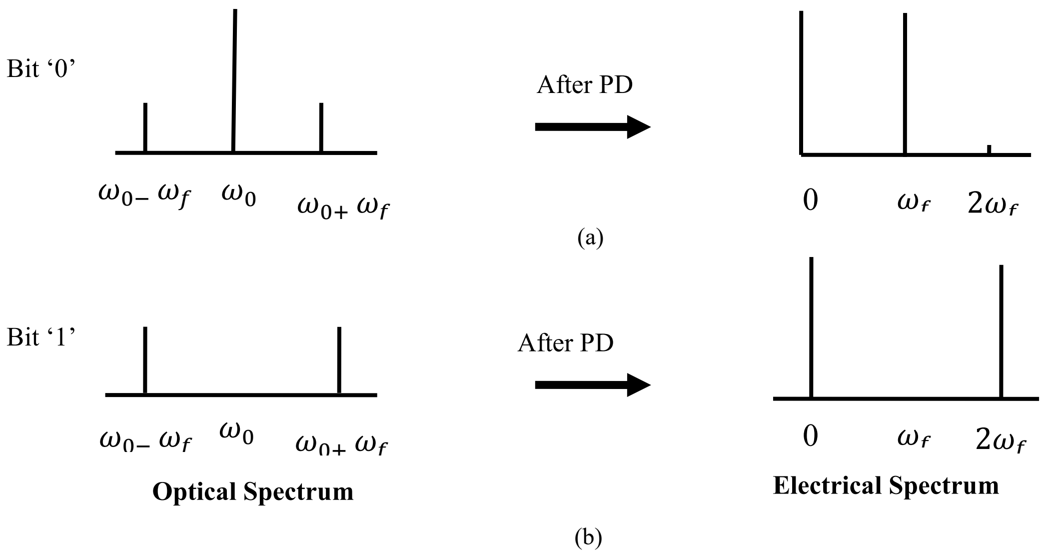

Fig. 3. Optical and electrical spectrum after photo detection for (a) bit '0' (b) bit '1'

The generated electrical output from RF stage is expressed as [11,12]:

$$E_{in} = b_0(t)A_{RF0}\cos(2\pi f_{RF}\ t) + b_1(t)A_{RF1}\cos(2\pi f_{RF}\ t) \tag{1}$$

where $b_0(t)$ and $b_1(t)$ are the bit '0' and '1' respectively of pseudo random bit sequence (PRBS) and A_{RF0} (for bit '0') and A_{RF1} (for bit '1') are the amplitudes of the generated electrical signal.

When MZM is biased for bit '0' at the quadrature point, the optical output signal is obtained by considering only the 1storder sidebands while neglecting the higher sidebands as shown in Fig. 3 (a) and is given below [12]:

$$E_{out0} = \frac{E_0\sqrt{2}}{2}\{J_0(\beta_1)\cos(\omega_0\ t) - J_1(\beta_1)\begin{matrix}(\omega_0+\omega_f)t+\\ [\cos\end{matrix}\ \cos(\omega_0 - \omega_f)t]\} \quad (2)$$

where the modulation index of the MZM is given by $\beta_1 = \pi V_{RF0}\frac{1}{2}V_\pi$ and V_π is the half-wave voltage, E_0 is the amplitude and ω_0 is the optical carrier angular frequency. The nth order Bessel function is denoted by J_n. At the end of the photodetector (PD), the detected electrical signal is given as [12]:

$$i_{out0} \propto \frac{E_0^2}{2}[-2J_0(\beta_1)\ J_1(\beta_1)\ \cos(\omega_f\ t) + J_1(\beta_1)^2\cos(2\omega_f\ t)] \quad (3)$$

When MZM is biased at the null point for bit ‘1’, the even-order sidebands are suppressed as shown in Fig. 3(b) and the carrier-less optical modulated signal is obtained. Thus, the output of MZM and electrical signal at end of the PD are expressed in equations 4 and 5 respectively as [12]:

$$E_{out1} = E_0\{-J_1(\beta_2)[\cos(\omega_0+\omega_f)t + [\cos(\omega_0 - \omega_f)t]\} \quad (4)$$

and

$$i_{out1} \propto E_0^2[J_1(\beta_2)^2\cos(2\omega_f\ t)] \quad (5)$$

where $\beta_2 = \pi V_{RF1}/2\ V_\pi$ is MZM modulation index.

The resultant amplitude V of the photodetector output is obtained by regulating the bias voltages and RF signal amplitudes of the MZM precisely and is given as [12]:

$$V = |J_0(\beta_1)J_1(\beta_1)| = J_1(\beta_2)^2 \gg \frac{J_1(\beta_1)^2}{2} \quad (6)$$

To satisfy the above equation (6), the RF signal magnitudes of the ‘0’ and ‘1’ bits is adjusted to $0.8\,V_\pi$ and $1.3V_\pi$ respectively. Therefore, the resultant generated electrical signal (refer equations 3 and 5) can be expressed as [12]:

$$i_{out} \propto |E_0|^2 A\cos(\omega_f t)\ldots \text{ for bit ‘0’}$$

$$i_{out} \propto |E_0|^2 A\cos(2\omega_f t)\ldots \text{ for bit ‘1’} \quad (7)$$

As can be observed from equation (7), the produced electrical signal angular frequencies for ‘0’ and ‘1’ bits are ω_f and 2ω respectively. Therefore, mm-wave FSK signal is generated successfully with f RF and f2RFfrequencies having same amplitude for ‘0’ and ‘1’bits.

3. Proposed design

Fig. 4 shows the system setup to realize millimeter-wave frequency upconversion using a MZM. Here, a single drive MZM based simple scheme is used to obtain tunable FSK millimeter-wave (20 – 60 GHz)to accomplish 5 G applications in FR2 millimeter-wave band (24.25-52.6 GHz).

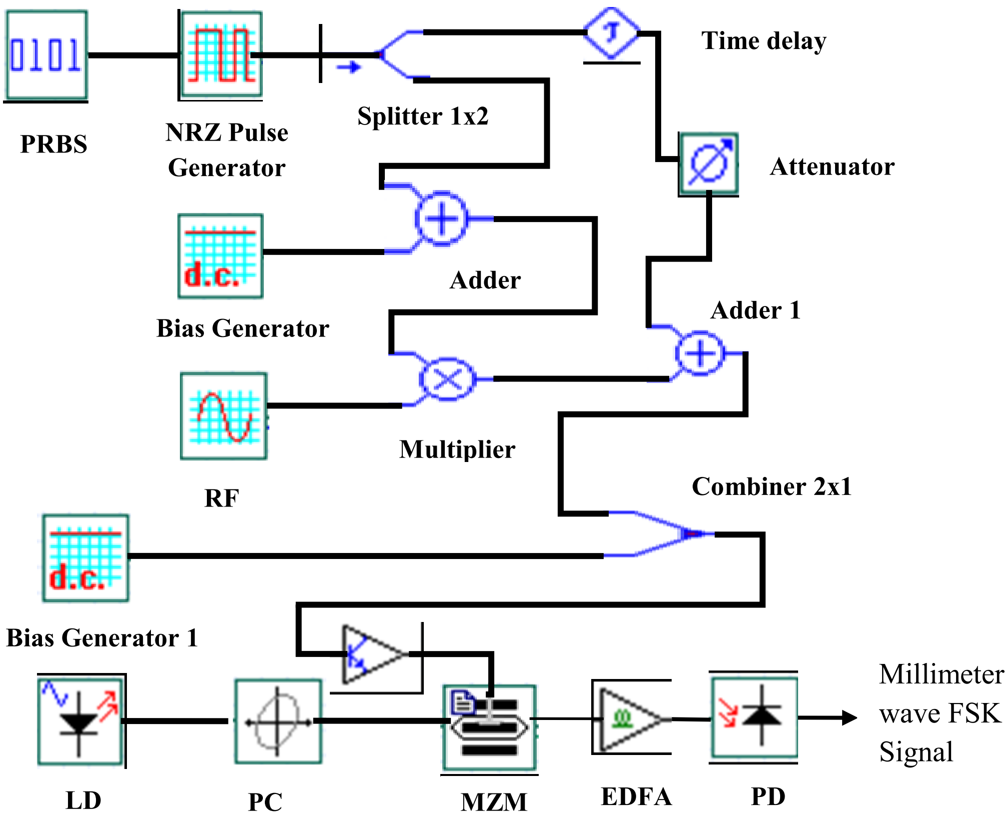

Fig. 4. System modelfor the photonic generation of FSK with MPM (colour online)

In this model, PRBS generator is used to generate on-off keying (OOK) bipolar non-return-to-zero (NRZ) electrical output with variable bit rate (2.5 Mb/s – 5 Gb/s) and this signal is separated into two sections through a splitter. Here, first section is joined with a DC input having an amplitude 1 a.u. to achieve the ASK output and after this, combined with varied RF signal (10, 20 and 30 GHz). Another part is attenuated and joined with mixer output, which has identical binary sequence as that of the ASK signal. Then, the signal biased at 0.5 a.u. is amplified with the help of electrical amplifier and is fed to MZM. Therefore, ‘0’ and ‘1’bits of the produced signal have distinct RF amplitude as well as DC components. Further, the electric delay line is used to synchronize OOK and ASK signals. A continuous-wave (CW) from optical laser at 1550 nm with input power of 5 dBm is transmitted to a single-drive MZM via 90 deg polarization controller (PC). The considered MZM parameters are: splitting ratio=1.3, bias voltage V1=-2.775 V and V2=-2.8125 V. With fine tuning of each signal amplitude as well as bias voltage of the MZM, millimeter-wave FSK signal with twice the RF signal frequency for distinct bit rates can be achieved. The 5 m EDFA is used before PD as a preamplifier to compensate for the modulator’s insertion loss. The photoelectrical conversion is carried out by photodetector with 1A/W responsivity and 0.9 ionization ratio. The detected electrical signal is examined using spectrum analyzer. The main parameters of the proposed model are tabulated in Table 1.

Table 1. Simulation parameters of various components of MPM of the proposed model

Component	Parameter	Values
LD	Frequency	1550 nm
	Power	5 dBm
PC	Phase	90 deg
Input	RF frequency	10,20 and 30 GHz
	DC bias amplitude	1 a.u, 0.5 a.u
	Bit rate for 10,20 and 30GHz	2.5 Gbps, 5 Gbps
MZM	Bias 1	-2.775 V
	Bias 2	-2.8125 V
	Modulation Voltage	1.2 V
	Splitting ratio	1.3
EDFA	Length	5 m
	Noise centre frequency	193.4T Hz
PD	Responsivity	1A/W
	Ionization ratio	0.9
	Shot noise	Yes
	Thermal noise	10e-24 W/Hz
	Dark current	10 nA

4. Results and discussion

In this work, the tunability of mm-wave FSK signal for 10, 20 and 30 GHz RF signal using 2.5 and 5 Gb/s has been investigated for upcoming 5G wireless applications. The Figs. 5, 6 and 7 represent the produced electrical signals, millimeter-wave FSK signals along with electrical frequency spectra of these signals using electrical and optical analyzers.

- ***Case 1 tunability of 10 GHz RF signal for 2.5 and 5Gb/s***

In the proposed scheme, an electrical outputis generated with two distinct RF amplitudes using input DC bias voltages for ‘0’ and ‘1’ bits. This signal is amplified and sent to single-drive MZM biased at the null and quadrature point of the transmission curve for ‘1’ and ‘0’ bits respectively. Because of the varying amplitude of RF signal, a millimeter-wave FSK signal is successfully generated having the space frequency identical to the frequency of RF signal (ωf) and the mark frequency double the RF signal ($2\omega f$).

Figs. 5(a) to 5(c) show the produced electrical outputs, millimeter-wave FSK signals and electrical frequency spectra considering RF clock frequency of 10 GHz for verifying the tunability at 2.5 and 5 Gb/s. Fig. 5(a) (i and ii) shows the generated electrical signals by using OOK modulation scheme where‘0’ and ‘1’ bits are represented with two distinct amplitude levels. Constant amplitude millimeter-wave FSK signals obtained after MZM are observed in Fig. 5(b) (i and ii) showing the variation in frequency for ‘0’ and ‘1’ bits. Modulated FSK signal frequency is doubled (ω_{2f} = 20 GHz) for mark i.e. bit ‘1’ and remains same (ω_f=10 GHz) for space i.e. bit ‘0’. The transition time for generated mm-wave FSK is about 0.4 ns. The electrical spectra of the photo detected signals are shown in Fig. 5(c) (i and ii) where two distinct peaks are clearly visible at 10 and 20 GHz (f_{RF} and $2f_{RF}$ respectively). It is also evident from the Fig. 5c (i and ii) that as the data rate is increased from 2.5 to 5 Gb/s, the spectrum expands due to the generation of high-power inter modulation (IM) frequencies. The IM frequencies lead to the inter-symbol interference (ISI) resulting in poor detection of the desired frequencies. For future 5 G wireless applications, the advanced digital filters and equalizers can further be employed to achieve better signal processing and its detection [17,18].

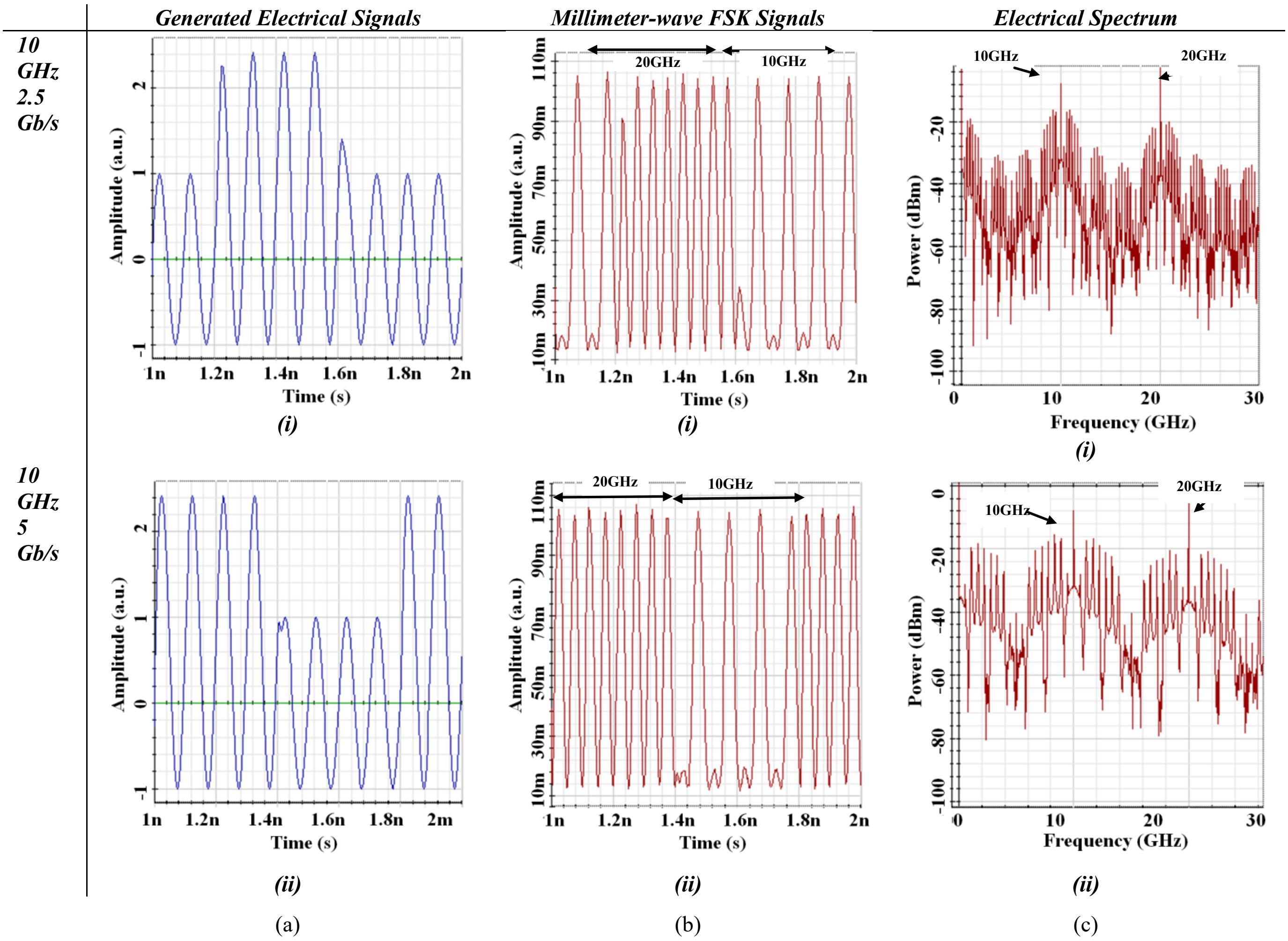

Fig. 5. Shows results of 10 GHz RF clock at bit rate 2.5 and 5 Gb/s (colour online)

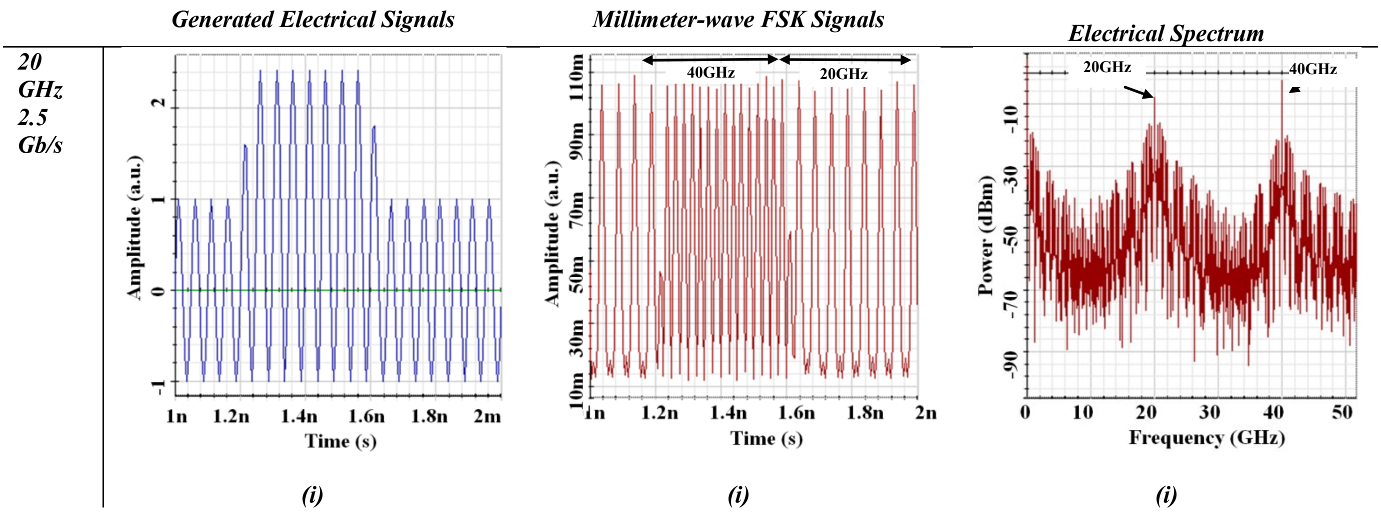

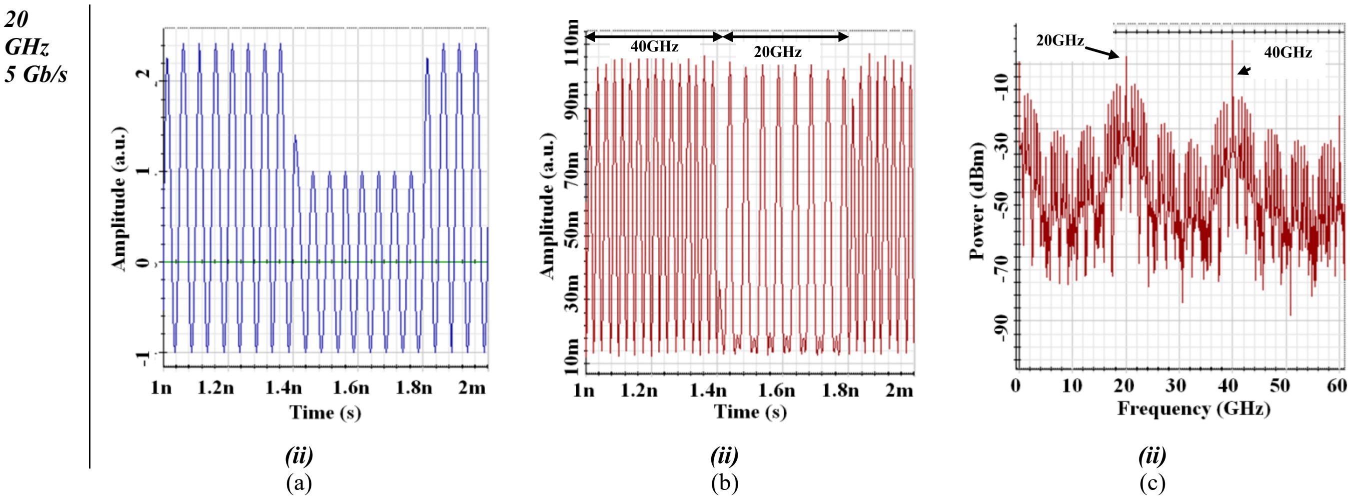

Fig. 6. Shows results of 20 GHz RF clock at bit rate (a) 625 Mb/s, (b) 1.25 Gb/s, (c) 2.5 Gb/s (colour online)

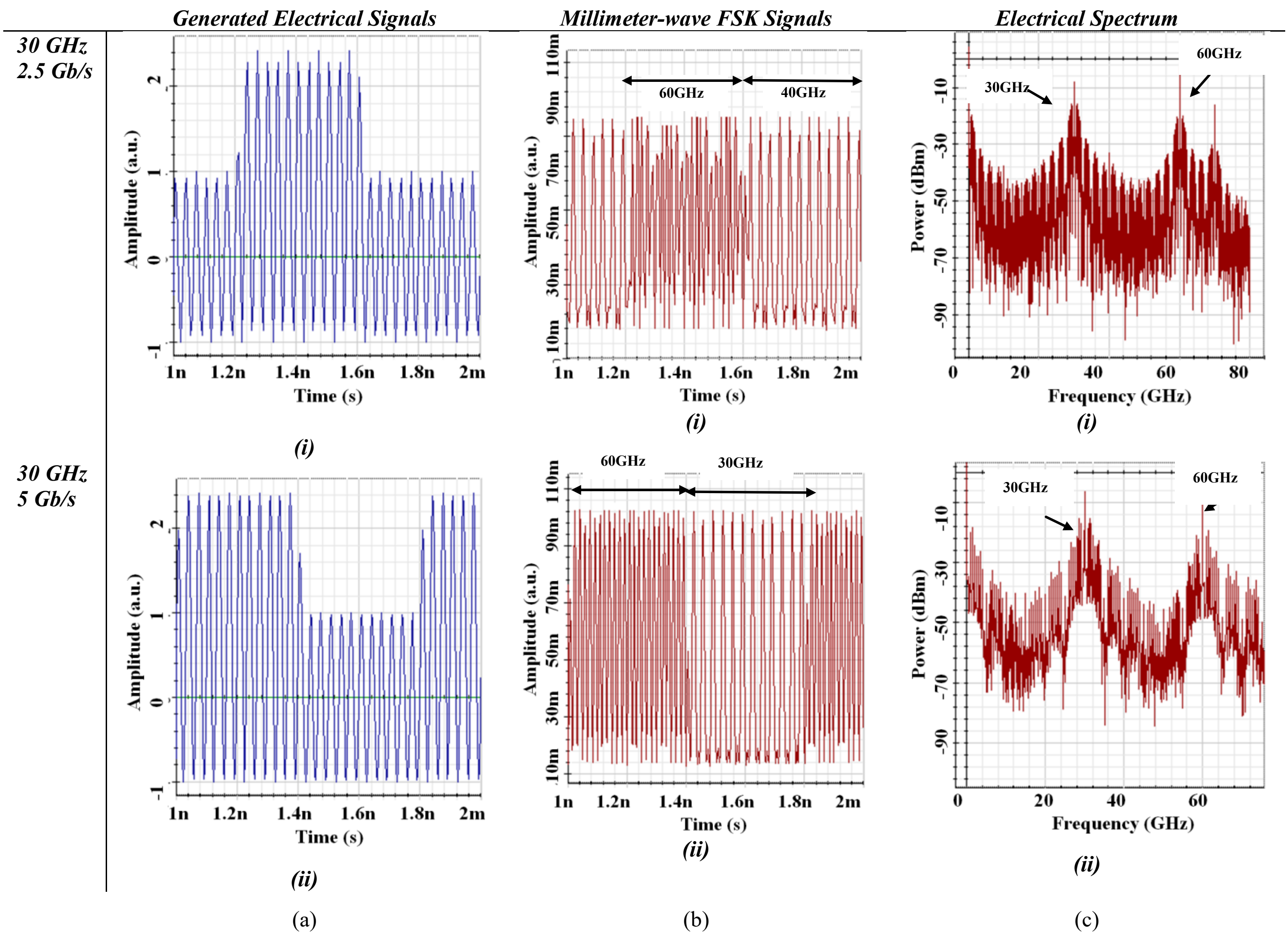

Fig. 7. Shows results of 10 GHz RF clock at bit rate 2.5 and 5 Gb/s (colour online)

- ***Case 2 tunability of 20 GHz RF signal for 2.5 and 5 Gb/s***

Fig. 6(a)-6(c) show produced electrical outputs, millimeter-wave FSK signals and electrical frequency spectra considering 20 GHz RF clock frequency tuned for 2.5 and 5 Gb/s. In Fig. 6(a) (i and ii), the generated electrical signals are shown for '0' and '1' bits by using OOK modulation. The generated mm-wave FSK signal with 0.4 ns transition time contains two frequencies ω_f = 20 GHz and ω_{2f} = 40 GHz for space and mark bits respectively as shown in Fig. 6(b) (i and ii). The spectra of photo detected electrical signal shows two distinct peaks at

20 and 40 GHz (f_{RF} and $2f_{RF}$) as depicted in Fig. 6(c) (i and ii)

- ***Case 3 tunability of 30 GHz RF signal for 2.5 and 5 Gb/s***

Fig. 7(a)-7(c) show the similar patterns of generated electrical signals, mm-wave FSK signals and electrical frequency spectra with 30 GHz RF clock frequency tuned at 2.5 and 5 Gb/s. As the data rate is increased from 2.5 to 5 Gb/s, the spectrum broadens due to the production of higher order IM harmonic frequencies. It is evident from the Fig. 7(c) (i and ii) that for 30 GHz RF frequency, the two frequencies ω_f (30 GHz) and ω_{2f} (60 GHz) are produced. Further, it is worth mentioning here that the electrical spectrum at 30 GHz RF signal has comparatively less IM distortion than 10 and 20 GHz. So, for 30 GHz signal the conventional digital filters can be employed for further signal conditioning and processing thus supporting in the realization of cost efficient 5 G wireless communications systems [19,20].

This 30 GHz RF signal is suitable for supporting ultra-wide NR FR2 band applications with the scope of expansion from V to W band (40-110 GHz) which will explore closely packed licensed/unlicensed spectrum utilization for back-/fronthaul networks, IoT systems, private network, vehicle-to-everything (V2X) and many more for future wireless devices. Table 2 depicts the superiority of the proposed work with existing ones [21].

Table 2. Comparative analysis w.r.t. existing works

Ref.	Data rate	Maximum Frequency	Millimeter Wave	Applications	Limitations
[11]	10 Gbps	25 GHz	-	WDM	Costly
[13]	-	10 KHz	ASK and FSK	Radars	Require tunable filters
[15]	20 Gbps	60 GHz	-	CMOS	Complex
[22]	10 Gbps	60 GHz	ASK, FSK, PSK, PSK, quadrature amplitude modulation	5G	Noise and errors
[14]	12 Kbps	24 GHz	BPSK	Radar	Costly
[23]	15 Gbps	80 GHz	-	5G	Limited distance
[4]	10 Gbps	100 GHz	ASK	Gas sensing	Limited throughput
[5]	12.5 Gbps	60 GHz	-	5G	Limited throughput
This work	2.5 Gbps, 5 Gbps	30 GHz	FSK	5G and Space	Limited throughput

5. Conclusion

To support the use of tightly coupled licensed and unlicensed NR-FR2 millimeter-wave band (24.25- 52.6 GHz) for future 5 G wireless applications, here, a new opportunity to access backhaul network is explored upto 60 GHz. In this model, the transmitter MZM biased at quadrature and null points is tuned for 2.5 and 5 Gb/s with varying RF clock (10-30 GHz) to generate mm-wave FSK signal. At the receiver, photodetector IF electrical signal with two frequencies ω_f (same as RF) and ω_{2f} (twice the RF) is obtained. It is observed the electrical spectra for 30 GHz RF clock show optimum results with comparatively less IM distortion than 10 and 20 GHz. Hence, 30 GHz signal with conventional digital filters can be employed for further signal processing resulting in cost efficient 5G wireless communications systems. Millimeter-wave incorporates very high frequency as well as large broadband realizing the data transmission with super large capacity upto 1 TGbps. The base station as well as radio antennas of the wireless networks utilizing the mm-wave technology, are compact, which is extremely useful for installation, maintenance as well as expansion. Moreover, mm-wave beam is quite narrow and thus has good directivity in wireless communication. It also offers reliable and relatively stable propagation with high safety factor. Although, with the increment in transmission distance and the continuous demand of system capacity, the mm-wave based system still has almost shortcomings, and there are even many unfamiliar terrain to be explored. This paper is expected to be helpful in realizing mm-wave 5 G applications with simple structure and high tunability.

References

[1] B. C. Henderson, Watkins-Johnson Co. Tech-Notes **17**, 1 (1990).
[2] A. J. Seeds, K. J. Williams, J. Light. Technol. **65**, 4628 (2022).
[3] J. Yao, Photonics Soc. Newsl. **24**, 4 (2012).
[4] Y. Kado, T. Nagatsuma, Prog. Electromagn. Res. Symp. **1**, 32 (2009).
[5] N. J. Gomes, M. Morant, A. Alphones, B. Cabon, J.

E. Mitchell, C. Lethien, M. Csörnyei, A. Stöhr, S. Iezekiel, J. Opt. Netw. **8**, 156 (2009).
[6] Z. Li, W. Li, H. Chi, X. Zhang, J. Yao, IEEE Photonics Technol. Lett. **23**, 712 (2011).
[7] Y. Zhang, S. Pan, Opt. Lett. **38**, 766 (2013).
[8] Z. Li, H. Chi, X. Zhang, J. Yao, IEEE Photonics Technol. Lett. **23**, 558 (2011).
[9] R. Wu, C. M. Long, D. E. Leaird, A. M. Weiner, IEEE Photonics Technol. Lett. **24**, 1484 (2012).
[10] W. Li, J. Yao, Opt. Express **21**, 15692 (2013).
[11] J. Wu, P. Cao, T. Pan, Y. Yang, C. Qiu, C. Tremblay, Y. Su, Photonics Res. **3**, 9 (2015).
[12] J. Xiao, C. Zhao, X. Feng, X. Dong, J. Zuo, J. Ming, Y. Zhou, Adv. Condens. Matter. Phys. **2020**, 6692941 (2020).
[13] N. Iu, X. S. T. Y. Ao, Opt. Express **32**, 39643 (2024).
[14] N. Souzandeh, M. Harifi-Mood, S. Aissa, S. O. Tatu, IEEE Access **12**, 129776 (2024).
[15] Y. Liang, Y. Zhang, K. Yang, Z. Li, G. Zhong, L. Lian, 2024 Photonics Electromagn. Res. Symp. PIERS 2024 - Proc. 1 (2024).
[16] S. E. Alavi, M. R. K. Soltanian, I. S. Amiri, M. Khalily, A. S. M. Supa'At, H. Ahmad, Sci. Rep. **6**, Article number: 19891 (2016).
[17] V. Arya, J. Opt. Commun. https://doi.org/10.1515/joc-2025-0008 (2025).
[18] H. Singh, 2021 2nd Int. Conf. Smart Electron. Commun. 1722 (2021).
[19] H. Singh, Mater. Today Proc. **37**, 3615 (2021).
[20] H. Singh, Ba. S. Sohi, A. Gupta, Int. J. Electron. **108**, 1035 (2021).
[21] H. Singh, B. S. Sohi, A. Gupta, J. Sci. Ind. Res. **79**, 297 (2020).
[22] A. Sindhiya, P. E. Irin Dorathy, Int. Res. J. Eng. Technol. **9**, 2149 (2022).
[23] S. Dahiya, Asha, J. Opt. **53**, 2174 (2024).

*Corresponding author: meetkumari08@yahoo.in